Available online at www.derpharmachemica.com

ISSN 0975-413X
CODEN (USA): PCHHAX

Der Pharma Chemica, 2016, 8(1):475-482
(http://derpharmachemica.com/archive.html)

A theoretical study of the inhibition of human 4-hydroxyphenylpyruvate dioxygenase by a series of pyrazalone-quinazolone hybrids

Juan S. Gómez-Jeria* and Camila Moreno-Rojas

Quantum Pharmacology Unit, Department of Chemistry, Faculty of Sciences, University of Chile. Las Palmeras 3425, Santiago, Chile

---

ABSTRACT

A Density Functional Theory study was carried out to find relationships between the electronic/molecular structure of a group of pyrazalone-quinazolone hybrids and their inhibition of human 4-hydroxyphenylpyruvate dioxygenase (HPPD). The geometries were fully optimized at the B3LYP/6-31G(d,p) level. A statistically significant equation was obtained. The equivalent 2D pharmacophore was built and some atom-site interactions were suggested. The analysis of the equation and the pharmacophore should provide new information about possible substitution sites for an enhancing of the inhibitory activity.

Keywords: HPPD, 4-hydroxyphenylpyruvate dioxygenase, QSAR, DFT calculations, reactivity indices, inhibition constant, electronic structure.

INTRODUCTION

In aerobic metabolism, the conversion of 4-hydroxyphenylpyruvate into 2,5 dihydroxyphenylacetate (homogentisate) is catalyzed by the enzyme 4-hydroxyphenylpyruvate dioxygenase (HPPD). In animals this pathway is required to control blood tyrosine levels. In *Homo sapiens*, the abnormal metabolism in the tyrosine catabolism pathway gives rise to various diseases, such as Type I tyrosinemia, Type II tyrosinemia, Type III tyrosinemia, hawkinsinuria and alkaptonuria (alcaptonuria, black urine disease or black bone disease). HPPD is linked directly to alkaptonuria (a deficiency in active homogentisate 1,2-dioxygenase), Type III tyrosinemia (a deficiency of active HPPD) and hawkinsuremia (a result of uncoupled turnover of HPPD). The specific inhibition of HPPD can relieve the symptoms of alkaptonuria, Type I tyrosinemia and perhaps hawkinsinuria, by ending the flux of metabolites through four of the five steps of tyrosine catabolism. Also, naturally occurring allelopathic diketone and triketone alkaloids inhibit HPPD in a specific way which prevents the creation of homogentisate and consequently the synthesis of tocopherols and plastoquinones, the latter of which is vital for photosynthesis. Therefore, molecules that specifically inhibit HPPD have potential use as herbicides. Several groups of molecules have been synthesized and tested for HPPD inhibition [1-14]. Recently, Yang et al. synthesized a series of pyrazolone–quinazolone hybrids that are novel potent human HPPD inhibitors [3]. As a contribution for a better understanding the action mechanism of HPPD inhibitors, we present here the results of a study relating the electronic/molecular structure of the abovementioned molecules with their inhibition constants against recombinant human HPPD.

MATERIALS AND METHODS

The method

Considering that the formal model employed here has been presented in several papers [15-23], we shall present here only its main lines of development and discuss below only the results obtained here. Starting from the statistical-mechanical definition of the equilibrium constant, an expression relating this experimental value with several local atomic reactivity indices and orientational parameters was developed. This model is the sole member of the class of formal models. Its application to several different molecules and receptors gave very good results (see [23-38] and references therein). Its extension to all kinds of biological activities was very fruitful (see [38-52] and references therein).

Selection of biological activity

The molecules were selected from Ref. [3]. The chosen experimental values are the inhibition constants (K_i) against recombinant human HPPD. Both are shown in Fig. 1 and Table 1.

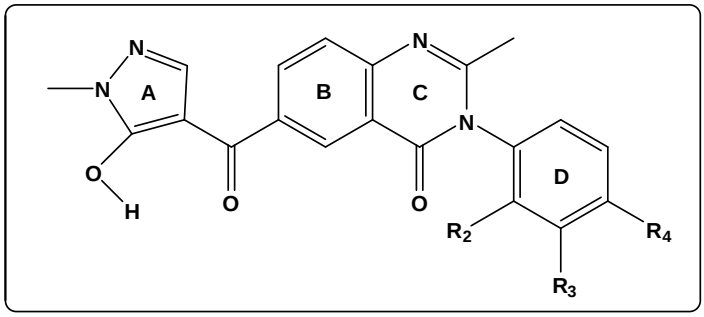

Figure 1. General formula of the selected pyrazalone-quinazolone hybrids

Table 1. Pyrazalone-quinazolone hybrids and HPPD inhibition constant (K_i)

Mol.	Mol.	R_2	R_3	R_4	log (K_I)
1	3a	H	H	H	1.28
2	3b	F	H	H	1.18
3	3c	Cl	H	H	1.34
4	3d	Br	H	H	1.38
5	3e	Me	H	H	1.76
6	3f	OMe	H	H	1.58
7	3g	H	F	H	1.30
8	3h	H	Cl	H	1.00
9	3i	H	Br	H	1.15
10	3j	H	Me	H	1.11
11	3k	H	OMe	H	1.53
12	3l	H	OCF_3	H	1.49
13	3m	H	H	F	1.53
14	3n	H	H	Cl	1.34
15	3o	H	H	Br	1.26
16	3p	H	H	Me	1.40
17	3q	H	H	OMe	1.78
18	3r	H	H	OCF_3	2.20
19	3s	Me	H	Cl	1.51
20	3t	Me	H	F	1.60
21	3u	Br	H	Me	1.04
22	3v	H	Cl	Cl	1.40
23	3w	F	H	Me	2.23
24	3x	Cl	H	Me	1.95
25	3y	Me	H	Me	1.77

Calculations

As usual, we worked within the common skeleton hypothesis asserting that there is a set of atoms, common to all the molecules analyzed, that explains practically all the biological activities. The effect of the substituents is to change

the electronic structure of the common skeleton and/or influencing the correct placement of the inhibitor molecule. The common skeleton is shown in Fig. 2, together with the atom numbering employed in the resultant statistical equations.

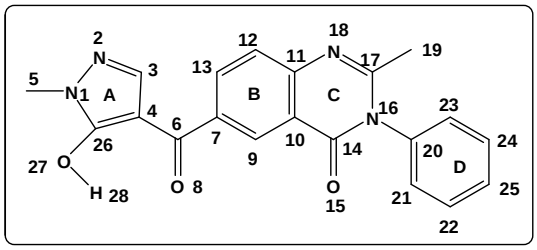

Figure 2. Common skeleton numbering

Molecular geometries were fully optimized at the B3LYP/6-31G(d,p) level of the theory with the Gaussian 03 suite of programs [53]. From the corrected Mulliken Population Analysis results [54], the numerical values for all electronic local atomic reactivity indices were obtained. The D-Cent-QSAR software was used [55]. The orientational parameters for the R_2-R_4 substituents were calculated with the Steric software [56]. As the system of linear equations cannot be solved because the number of molecules is smaller than the number of unknown coefficients, a linear multiple regression analysis (LMRA) was carried out. The Statistica software was used [57].

RESULTS

The best equation obtained with LMRA is:

$$\log(K_i) = 1.47 - 0.69F_1(HOMO-2)^* + 0.001\phi_{R4} + 6.92F_{17}(HOMO-2)^* + \\ +6.48F_{19}(LUMO+2)^* - 0.21S_5^N(LUMO+1)^* + 1.18F_{18}(HOMO-2)^* - \\ -2.50F_{14}(HOMO-1)^* \quad (1)$$

with n=25, R= 0.96, R^2= 0.92, adj. R^2= 0.89, F(7,17)=28.62 ($p<0.000001$) and a standard error of estimate of 0.11. No outliers were detected and no residuals fall outside the ±2σ limits. Here, $F_1(HOMO-2)^*$ is the Fukui index of the third highest occupied MO localized on atom 5, ϕ_{R4} is the orientational parameter of the R_4 substituent, $F_{17}(HOMO-2)^*$ is the Fukui index of the third highest occupied MO localized on atom 17, $F_{19}(LUMO+2)^*$ is the Fukui index of the third vacant MO localized on atom 19, is $S_5^N(LUMO+1)^*$ the nucleophilic superdelocalizability of the second vacant MO localized on atom 5, $F_{18}(HOMO-2)^*$ is the Fukui index of the third highest occupied MO localized on atom 18 and $F_{14}(HOMO-1)^*$ is the Fukui index of the second highest occupied MO localized on atom 14 (see Fig. 2). Table 2 shows the beta coefficients and the results of the t-test for significance of coefficients of Eq. 1. Table 3 displays the squared correlation coefficients for the variables appearing in Eq. 1. With the exception of two reactivity indices belonging atoms 5 and 19 (Fig. 2) showing a 32% correlation, there are no important internal correlations. Note that these two atoms are separated by a long distance. Fig. 3 displays the plot of observed *vs.* calculated log (K_i) values. The associated statistical parameters of Eq. 1 indicate that this equation is statistically significant and that the variation of the numerical value of a set of seven local atomic reactivity indices of atoms belonging to the common skeleton explains about 89% of the variation of the HPPD inhibition constant.

Table 2. Beta coefficients and *t*-test for significance of the coefficients in Eq. 1

	Beta	ID VAR	t(17)	p-level
Var5	-0.38	$F_1(HOMO-2)^*$	-4.62	<0.0002
Var564	0.53	ϕ_{R4}	7.50	<0.000001
Var325	0.41	$F_{17}(HOMO-2)^*$	5.25	<0.00007
Var370	0.58	$F_{19}(LUMO+2)^*$	5.62	<0.00003
Var95	-0.46	$S_5^N(LUMO+1)^*$	-4.69	<0.0002
Var345	0.27	$F_{18}(HOMO-2)^*$	3.34	<0.004
Var266	-0.19	$F_{14}(HOMO-1)^*$	-2.56	<0.02

Table 3. Squared correlation coefficients for the variables appearing in Eq. 1

	$F_1(HOMO-2)^*$	ϕ_{R4}	$F_{17}(HOMO-2)^*$	$F_{19}(LUMO+2)^*$	$S_5^N(LUMO+1)^*$	$F_{18}(HOMO-2)^*$
ϕ_{R4}	0.01	1.00				
$F_{17}(HOMO-2)^*$	0.06	0.00	1.00			
$F_{19}(LUMO+2)^*$	0.12	0.005	0.03	1.00		
$S_5^N(LUMO+1)^*$	0.002	0.004	0.10	0.32	1.00	
$F_{18}(HOMO-2)^*$	0.0004	0.05	0.06	0.07	0.004	1.00
$F_{14}(HOMO-1)^*$	0.03	0.002	0.05	0.01	0.02	0.06

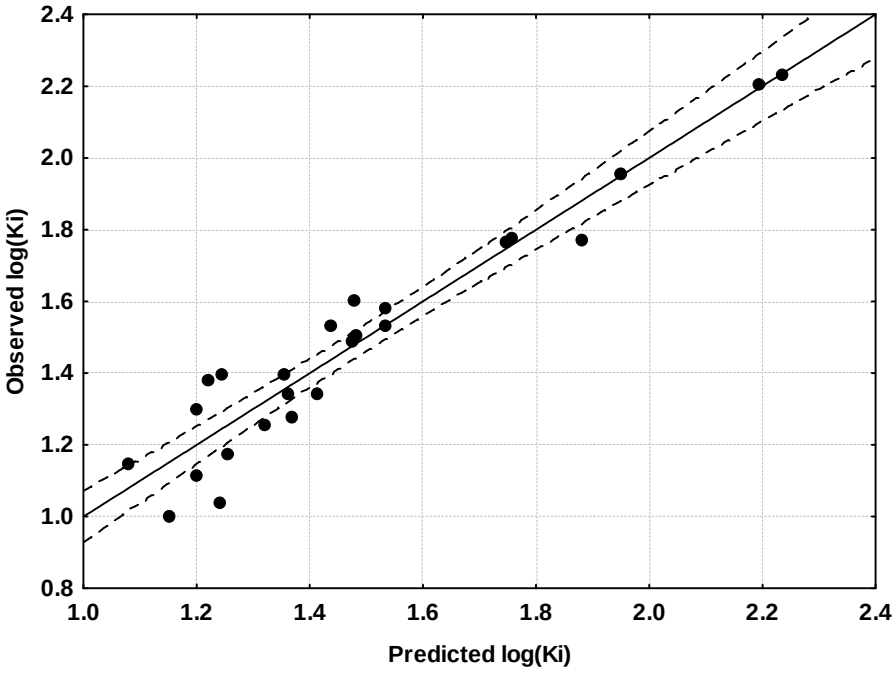

Figure 3. Observed *versus* calculated values (Eq. 1) of log (K_i). Dashed lines denote the 95% confidence interval

Local Molecular Orbitals

Tables 4 and 5 display the local molecular orbital structure of atoms appearing in Eq. 1 (Reading: molecule's number (HOMO)/ (HOMO-2)*, (HOMO-1)*, (HOMO)*- (LUMO)*, (LUMO+1)*, (LUMO+2)*).

Table 4. Local molecular orbital structure of atoms 1, 5 and 14

Mol.	Mol.	Atom 1(N)	Atom 5(C)	Atom 14(C)
1(94)	3A	92π93π94π-95π100π101π	78σ82σ92σ-104σ111σ112σ	89π90σ91σ-96π97π100π
2(98)	3B	96π97π98π-99π104π105π	84σ86σ96σ-108σ111σ115σ	94σ95σ97π-100π101π103π
3(102)	3C	100π101π102π-103π109π110π	86σ88σ100σ-13σ118σ120σ	96π97π98σ-104π105π107π
4(111)	3D	108π110π111π-112π118π119π	95σ97σ108σ-22σ127σ129σ	105σ106π107σ-113π114π116π
5(98)	3E	94π95π96π-99π101π102π	87σ94σ95σ-104σ113σ114σ	88π92σ97π-100π101π104π
6(102)	3F	98π99π101π-103π108π109π	88σ98σ99σ-108σ113σ121σ	98σ99σ102π-104π105π106π
7(98)	3G	96π97π98π-99π104π105π	82σ86σ96σ-108σ112σ116σ	90σ93σ94σ-100π101π102π
8(102)	3H	100π101π102π-103π109π110π	86σ88σ100σ-13σ117σ120σ	94σ97σ98σ-104π105π107π
9(111)	3I	108π110π111π-112π118π119π	93σ97σ108σ-22σ126σ129σ	101π106σ107σ-113π114π116π
10(98)	3J	95π97π98π-99π104π105π	81σ86σ95σ-108σ116σ117σ	89π93σ94σ-100π101π104π
11(102)	3K	99π100π102π-103π108π109π	85σ88σ99σ-108σ113σ121σ	93π97σ98σ-104π105π106π
12(114)	3L	112π113π114π-115π120π121π	99σ102σ112σ-124σ129σ132σ	109σ110σ111π-116π117π119π
13(98)	3M	95π97π98π-99π104π105π	83σ86σ95σ-108σ112σ115σ	93σ94σ96σ-100π102π103π
14(102)	3N	100π101π102π-103π109π110π	86σ88σ100σ-112σ113σ118σ	97σ98σ99σ-104π105π107π
15(111)	3O	108π110π111π-112π118π119π	95σ97σ108σ-121σ122σ127σ	106σ107σ109σ-113π114π116π
16(98)	3P	95π97π98π-99π104π105π	80σ86σ95σ-108σ114σ116σ	89π94σ96σ-100π101π102π
17(102)	3Q	99π100π102π-103π108π109π	85σ88σ99σ-108σ113σ117σ	93π98σ101σ-104π106π107π
18(114)	3R	112π113π114π-115π120π121π	99σ102σ112σ-124σ130σ132σ	109σ110σ111σ-116π118π119π
19(106)	3S	103π104π105π-107π111π113π	92σ93σ103σ-123σ124σ126σ	100σ102σ105π-108π109π113π
20(102)	3T	99π101π102π-103π108π102π	86σ89σ99σ-113σ116σ120σ	97σ100σ101π-104π105π107π
21(115)	3U	112π114π115π-116π122π123π	98σ101σ112σ-126σ131σ134σ	109σ110σ111σ-117π118π120π
22(110)	3V	108π109π110π-111π117π118π	92σ94σ108σ-121σ122σ126σ	106σ107σ109π-112π113π116π
23(102)	3W	100π101π102π-103π108π109π	86σ90σ99σ-112σ120σ121σ	95σ98σ101π-104π105π107π
24(106)	3X	104π105π106π-107π113π114π	88σ92σ103σ-117σ122σ125σ	100σ102σ104σ-108π109π111π
25(102)	3Y	98π99π100π-103π105π107π	87σ88σ98σ-108σ119σ120σ	96σ99σ101π-104π105π108π

Table 5. Local molecular orbital structure of atoms 17, 18 and 19

Mol.	Atom 17(C)	Atom 18(N)	Atom 19(C)
1(94)	91σ93π94π-95π97π98π	91π93π94π-95π96π98π	86σ90σ91σ-97σ98σ103σ
2(98)	95π97π98π-99π101π102π	96π97π98π-99π100π101π	90σ91σ95σ-106σ111σ114σ
3(102)	99σ101π102π-103π105π107π	99π101π102π-103π104π105π	90σ95σ99σ-107σ117σ119σ
4(111)	107σ110π111π112π114π116π	109π110π111π-112π113π116π	103σ104σ105σ-116σ120σ126σ
5(98)	93σ96π97π-99π100π101π	95π96π97π-99π100π101π	90σ92σ93σ-110σ114σ117σ
6(102)	100σ101π102π-103π105π106π	100π101π102π-104π105π106π	94σ96σ97σ-106σ110σ119σ
7(98)	95σ97π98π-99π101π102π	95π97π98π-99π100π102π	91σ93σ95σ-103σ106σ112σ
8(102)	97σ101π102π-103π105π107π	99π101π102π-103π104π107π	94σ95σ97σ-107σ111σ118σ
9(111)	106σ110π111π-112π114π116π	109π110π111π-112π113π116π	103σ104σ106σ-116σ120σ127σ
10(98)	93σ97π98π-99π101π102π	96π97π98π-99π100π101π	90σ93σ96σ-103σ106σ113σ
11(102)	100π101π102π-103π105π106π	100π101π102π-103π104π106π	94σ97σ98σ-106σ119σ120σ
12(114)	111σ113π114π-115π117π118π	111π113π114π-115π116π119π	106σ107σ109σ-119σ130σ131σ
13(98)	96σ97π98π-99π102π103π	96π97π98π-99π100π103π	93σ94σ96σ-103σ106σ112σ
14(102)	99σ101π102π-103π105π107π	99π101π102π-103π104π107π	94σ97σ99σ-107σ111σ119σ
15(111)	109σ110π111π-112π114π116π	109π110π111π-112π113π116π	106σ107σ109σ-116σ120σ128σ
16(98)	96σ97π98π-99π101π102π	96π97π98π-99π100π102π	90σ94σ96σ-103σ106σ115σ
17(102)	100π101σ102π-103π105π106π	100π101π102π-103π104π105π	91σ94σ98σ-106σ110σ119σ
18(114)	111σ113π114π-115π118π119π	112π113π114π-115π116π118π	106σ109σ111σ-119σ122σ129σ
19(106)	102σ104π105π-107π108π109π	102π104π105π-107π108π109π	100σ101σ102σ-118σ122σ125σ
20(102)	100σ101π102π-103π105π106π	100π101π102π-103π104π105π	96σ98σ100σ-105σ116σ117σ
21(115)	113σ114π115π-116π118π119π	113π114π115π-116π117π120π	107σ109σ110σ-120σ124σ133σ
22(110)	107σ109π110π-111π113π116π	107π109π110π-111π112π116π	103σ105σ107σ-116σ120σ126σ
23(102)	100σ101π102π-103π105π106π	100π101π102π-103π104π105π	94σ95σ100σ-110σ120σ121σ
24(106)	104σ105π106π-107π109π110π	104π105π106π-107π108π109π	99σ100σ104σ-111σ125σ126σ
25(102)	99σ100π101π-103π104π105π	99π100π101π-103π104π105π	94σ96σ97σ-122σ123σ124σ

DISCUSSION

Figure 4 shows the fully optimized structure of molecule 2. The most important fact to notice is that rings A, B-C and D are not coplanar. Therefore, the direct effect of the substituents of ring D on the electronic structure cannot propagate to the rest of the system.

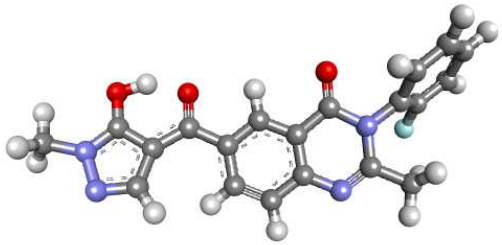

Fig 4. Fully optimized structure of molecule 2

Nevertheless, there is a second effect of the substituent that can alter the electronic structure. This effect is related to the appearance of new molecular orbitals that can alter the energy and/or location of the other MOs (a basis set effect). Table 2 shows that the importance of variables in Eq. 1 is $F_{19}(LUMO+2)^*$> ϕ_{R4}> $S_5^N(LUMO+1)^*$> $F_{17}(HOMO-2)^*$> $F_1(HOMO-2)^*$>>> $F_{18}(HOMO-2)^*$> $F_{14}(HOMO-1)^*$. A high inhibitory activity is associated with a small orientational parameter value for R_4, a high values for $F_{14}(HOMO-1)^*$ and $F_1(HOMO-2)^*$, low values for $F_{17}(HOMO-2)^*$, $F_{19}(LUMO+2)^*$ and $F_{18}(HOMO-2)^*$. The case of $S_5^N(LUMO+1)^*$ will be discussed below. Atom 1 is a nitrogen in ring A (Fig. 2). The three highest occupied and the three lowest vacant local MOs have a π nature (Table 4). A high value for $F_1(HOMO-2)^*$ suggests that atom1 is interacting with an electron-deficient center through its three highest occupied MOs. Atom 5 is the carbon of the methyl group attached to N1 in ring A (Fig. 2). All MOs have σ nature (Table 4). If the numerical values of $S_5^N(LUMO+1)^*$ are positive, then a high inhibitory activity is associated with high values for this index. To obtain high values, the corresponding MO energy must be shifted downwards, making this MO more reactive. This suggests that atom 5 is interacting with a rich electron center through at least its first two lowest vacant MOs. It is probably that the center has occupied σ MOs. Atom 17 is a carbon in ring C (Fig. 2). A high inhibitory activity is related to low numerical values of $F_{17}(HOMO-2)^*$. Table 5 shows that almost all $(HOMO-2)_{17}^*$ are of σ nature, while all $(HOMO-1)_{17}^*$ and $(HOMO)_{17}^*$ have a π nature. This suggests that this σ MO can difficult the interaction of $(HOMO-1)_{17}^*$ and $(HOMO)_{17}^*$ with an electron-deficient center. Atom 19 is a carbon of the methyl group attached to C17 (Fig. 2). All MOs have a σ nature (Table 5). A high inhibitory activity is associated with low numerical values for $F_{19}(LUMO+2)^*$. We tentatively suggest that this atom is interacting with an electron rich center with σ or π MOs. Atom 18 is a nitrogen in ring C (Fig. 2). The three highest occupied and the three lowest vacant local MOs have a π nature (Table 5). A high activity is associated with low values for $F_{18}(HOMO-2)^*$. Accordingly, we suggest that atom 18 is interacting with an electron deficient center (with π electrons) through its first two highest occupied MOs. Atom 14 is a carbon in ring B (Fig. 2). A high inhibitory activity is associated with high numerical values for $F_{14}(HOMO-1)^*$. Table 4 shows that the nature of $(HOMO-1)_{14}^*$ and $(HOMO)_{14}^*$ can be π or σ. The only suggestion is that atom 14 is interacting with an electron deficient center allowing interactions with σ and π electrons. A high inhibitory activity is associated with low ϕ_{R4} values [18, 22, 23]. This means that in the actual set under analysis a methyl substituent is the best choice. If this is true, then we could replace it by a substituent having the same effects on the electronic structure of ring D. The choice in this case is an ethyl group. All the above suggestion are summarized in the 2D corresponding pharmacophore shown in Fig. 5.

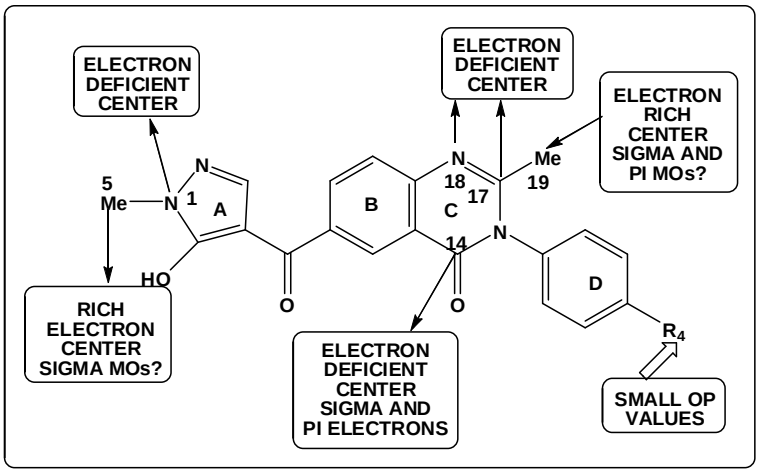

Figure 5. 2D pharmacophore for HPPD inhibition

In summary, we obtained a statistically significant relationship between the variation of the HPPD inhibition constant and the variation of the numerical values of six local atoms reactivity indices and of the orientational parameter of one of the substituents in a series of pyrazalone-quinazolone hybrids. The associated pharmacophore should provide information to develop new molecules with enhanced inhibitory activity.

REFERENCES

[1]K Lei, X-W Hua, Y-Y Tao, Y Liu, N Liu, et al., *Bioorg. Med. Chem.*, **2016**, 24, 92-103.
[2]Y-L Xu, H-Y Lin, X Ruan, S-G Yang, G-F Hao, et al., *Eur. J. Med. Chem.*, **2015**, 92, 427-438.
[3]Y-L Xu, H-Y Lin, R-J Cao, Z-Z Ming, W-C Yang, et al., *Bioorg. Med. Chem.*, **2014**, 22, 5194-5211.
[4]R Beaudegnies, AJF Edmunds, TEM Fraser, RG Hall, TR Hawkes, et al., *Bioorg. Med. Chem.*, **2009**, 17, 4134-4152.
[5]JA Conrad, GR Moran, *Inorg. Chim. Acta*, **2008**, 361, 1197-1201.
[6]D-W Wang, H-Y Lin, R-J Cao, T Chen, F-X Wu, et al., *J. Agric. Food. Chem.*, **2007**, 63, 5587-5596.
[7]LC Debra, HP Marshall, "A Structure-Based Design Approach to Plant Selective 4-Hydroxyphenylpyruvate Dioxygenase Inhibitors," in *Synthesis and Chemistry of Agrochemicals VII*, vol. 948, pp. 105-117, American Chemical Society, **2007**.
[8]GR Moran, VM Purpero, K Johnson, M Kavana, *J. Inorg. Biochem.*, **2003**, 96, 194.
[9]J-L Huang, H-G Liu, D-Y Yang, *Bioorg. Med. Chem. Lett.*, **2003**, 13, 927-930.
[10]Y-L Lin, C-S Wu, S-W Lin, J-L Huang, Y-S Sun, et al., *Bioorg. Med. Chem.*, **2002**, 10, 685-690.
[11]Y-L Lin, J-L Huang, C-S Wu, H-G Liu, D-Y Yang, *Bioorg. Med. Chem. Lett.*, **2002**, 12, 1709-1713.
[12]S-W Lin, Y-L Lin, T-C Lin, D-Y Yang, *Bioorg. Med. Chem. Lett.*, **2000**, 10, 1297-1298.
[13]T-s Ling, S Shiu, D-y Yang, *Bioorg. Med. Chem.*, **1999**, 7, 1459-1465.
[14]MK Ellis, AC Whitfield, LA Gowans, TR Auton, WM Provan, et al., *Toxicol. App. Pharmacol.*, **1995**, 133, 12-19.
[15]JS Gómez-Jeria, *Canad. Chem. Trans.*, **2013**, 1, 25-55.
[16]JS Gómez-Jeria, *Elements of Molecular Electronic Pharmacology (in Spanish)*, Ediciones Sokar, Santiago de Chile, 2013.
[17]T Bruna-Larenas, JS Gómez-Jeria, *Int. J. Med. Chem.*, **2012**, 2012 Article ID 682495, 1-16.
[18]JS Gómez-Jeria, M Ojeda-Vergara, *J. Chil. Chem. Soc.*, **2003**, 48, 119-124.
[19]JS Gómez-Jeria, "Modeling the Drug-Receptor Interaction in Quantum Pharmacology," in *Molecules in Physics, Chemistry, and Biology*, J. Maruani Ed., vol. 4, pp. 215-231, Springer Netherlands, **1989**.
[20]JS Gómez-Jeria, *Int. J. Quant. Chem.*, **1983**, 23, 1969-1972.
[21]F Peradejordi, AN Martin, A Cammarata, *J. Pharm. Sci.*, **1971**, 60, 576-582.
[22]JS Gómez-Jeria, *Res. J. Pharmac. Biol. Chem. Sci.*, **2016**, in press,
[23]JS Gómez-Jeria, M Ojeda-Vergara, C Donoso-Espinoza, *Mol. Engn.*, **1995**, 5, 391-401.
[24]MS Leal, A Robles-Navarro, JS Gómez-Jeria, *Der Pharm. Lett.*, **2015**, 7, 54-66.

[25]JS Gómez-Jeria, J Valdebenito-Gamboa, *Res. J. Pharmac. Biol. Chem. Sci*., **2015**, 6, 203-218.
[26]JS Gómez-Jeria, J Valdebenito-Gamboa, *Der Pharma Chem*., **2015**, 7, 323-347.
[27]JS Gómez-Jeria, A Robles-Navarro, *Res. J. Pharmac. Biol. Chem. Sci*., **2015**, 6, 1358-1373.
[28]JS Gómez-Jeria, A Robles-Navarro, *Res. J. Pharmac. Biol. Chem. Sci*., **2015**, 6, 1811-1841.
[29]JS Gómez-Jeria, A Robles-Navarro, *J. Comput. Methods Drug Des*., **2015**, 5, 15-26.
[30]JS Gómez-Jeria, *J. Chil. Chem. Soc*., **2010**, 55, 381-384.
[31]JS Gómez-Jeria, F Soto-Morales, J Rivas, A Sotomayor, *J. Chil. Chem. Soc*., **2008**, 53, 1393-1399.
[32]JS Gómez-Jeria, LA Gerli-Candia, SM Hurtado, *J. Chil. Chem. Soc*., **2004**, 49, 307-312.
[33]JS Gómez-Jeria, F Soto-Morales, G Larenas-Gutierrez, *Ir. Int. J. Sci*., **2003**, 4, 151-164.
[34]JS Gómez-Jeria, L Lagos-Arancibia, *Int. J. Quant. Chem.*, **1999**, 71, 505-511.
[35] JS Gómez-Jeria, D Morales-Lagos, JI Rodriguez-Gatica, JC Saavedra-Aguilar, *Int. J. Quant. Chem.*, **1985**, 28, 421-428.
[36]JS Gómez-Jeria, DR Morales-Lagos, *J. Pharm. Sci*., **1984**, 73, 1725-1728.
[37]JS Gómez-Jeria, D Morales-Lagos, "The mode of binding of phenylalkylamines to the Serotonergic Receptor," in *QSAR in design of Bioactive Drugs*, M. Kuchar Ed., pp. 145-173, Prous, J.R., Barcelona, Spain, **1984**.
[38]A Robles-Navarro, JS Gómez-Jeria, *Der Pharma Chem.*, **2016**, in press,
[39]JS Gómez-Jeria, J Valdebenito-Gamboa, *Der Pharma Chem*., **2015**, 7, 103-121.
[40]JS Gómez-Jeria, A Robles-Navarro, *Res. J. Pharmac. Biol. Chem. Sci*., **2015**, 6, 755-783.
[41]JS Gómez-Jeria, A Robles-Navarro, *Res. J. Pharmac. Biol. Chem. Sci*., **2015**, 6, 1337-1351.
[42]JS Gómez-Jeria, MB Becerra-Ruiz, *Der Pharma Chem.*, **2015**, 7, 362-369.
[43]DI Pino-Ramírez, JS Gómez-Jeria, *Amer. Chem. Sci. J.*, **2014**, 4, 554-575.
[44]D Muñoz-Gacitúa, JS Gómez-Jeria, *J. Comput. Methods Drug Des.*, **2014**, 4, 48-63.
[45]D Muñoz-Gacitúa, JS Gómez-Jeria, *J. Comput. Methods Drug Des.*, **2014**, 4, 33-47.
[46]JS Gómez-Jeria, *Res. J. Pharmac. Biol. Chem. Sci*., **2014**, 5, 780-792.
[47]JS Gómez-Jeria, *J. Comput. Methods Drug Des.*, **2014**, 4, 32-44.
[48]JS Gómez-Jeria, *Der Pharma Chem.*, **2014**, 6, 64-77.
[49]I Reyes-Díaz, JS Gómez-Jeria, *J. Comput. Methods Drug Des.*, **2013**, 3, 11-21.
[50]A Paz de la Vega, DA Alarcón, JS Gómez-Jeria, *J. Chil. Chem. Soc*., **2013**, 58, 1842-1851.
[51]JS Gómez-Jeria, M Flores-Catalán, *Canad. Chem. Trans*., **2013**, 1, 215-237.
[52]C Barahona-Urbina, S Nuñez-Gonzalez, JS Gómez-Jeria, *J. Chil. Chem. Soc.*, **2012**, 57, 1497-1503.
[53]MJ Frisch, GW Trucks, HB Schlegel, GE Scuseria, MA Robb, et al., "G03 Rev. E.01," Gaussian, Pittsburgh, PA, USA, **2007**.
[54] JS Gómez-Jeria, *J. Chil. Chem. Soc.*, **2009**, 54, 482-485.
[55] JS Gómez-Jeria, "D-Cent-QSAR: A program to generate Local Atomic Reactivity Indices from Gaussian 03 log files. v. 1.0," Santiago, Chile, **2014**.
[56]JS Gómez-Jeria, "STERIC: A program for calculating the Orientational Parameters of the substituents " Santiago, Chile, **2015**.
[57] Statsoft, "Statistica v. 8.0," 2300 East 14 th St. Tulsa, OK 74104, USA, **1984**-**2007**.